



## Research Article

# Dispersion model of NO<sub>x</sub> emissions from a liquefied natural gas facility

İlker TÜRKYILMAZ<sup>1</sup>, S. Levent KUZU<sup>2</sup>

<sup>1</sup>Department of Environmental Engineering, Yıldız Technical University, İstanbul, Türkiye

<sup>2</sup>Department of Environmental Engineering, İstanbul Technical University, İstanbul, Türkiye

## ARTICLE INFO

### Article history

Received: 09 January 2024

Revised: 20 February 2024

Accepted: 27 February 2024

### Key words:

AERMOD; Dispersion model;  
Emissions; Liquefied natural gas

## ABSTRACT

Natural gas is widely used in energy production, one of the most prominent sectors for human-kind. Combustion processes inevitably produce air pollutants. The major pollutant during a combustion process is nitrogen oxide emissions. The term of nitrogen oxides primarily include nitrogen monoxide and nitrogen dioxide. These pollutants are generated regardless of the fuel content since air composition itself is the major source for these pollutants. It is possible to calculate emissions through the activity data and emission factors. Calculation of emissions is not enough for an environmental assessment. The impact of pollutants on human health relies on their concentration in the atmosphere. In order to determine their concentrations several modelling practices are developed. In this study, AERMOD used for modelling purpose of NO<sub>x</sub> emissions from a liquefied natural gas facility. It was observed that the pollutants were dispersed mostly towards south-southwest of the facility, where Marmaraeğlisi district is located. Although the pollutants transported directly to the settlement, the concentrations remained limited. During operation conditions, the highest daily NO<sub>x</sub> concentration was 1.7 µg/m<sup>3</sup> and the highest annual concentration was 0.1 µg/m<sup>3</sup>. At maximum operating conditions, the highest daily NO<sub>x</sub> concentration was 16.2 µg/m<sup>3</sup> and the highest annual concentration was 2.5 µg/m<sup>3</sup>. At minimum operating conditions, the highest daily NO<sub>x</sub> concentration was 1.1 µg/m<sup>3</sup> and the highest annual concentration was 0.2 µg/m<sup>3</sup>.

**Cite this article as:** Türkyılmaz İ, Kuzu SL. Dispersion model of NO<sub>x</sub> emissions from a liquefied natural gas facility. Environ Res Tec 2024;7(X)00–00.

## INTRODUCTION

Air pollution modeling is a numerical tool used to understand the relationship between emissions, meteorology, atmospheric concentrations, soil deposition, and other factors. These models can identify causes and solutions to air quality problems that air pollution measurements cannot provide. Air pollution models can quantitatively evaluate the relationships between emissions and atmospheric concentrations and accumulations, thereby determining the consequences of past and future scenarios as well as the effectiveness of mitigation strategies. These

models are indispensable in scientific, regulatory and research practices. The concentrations of substances in the atmosphere are determined by the processes of transport, diffusion, chemical transformation and accumulation. While transport phenomena have been studied for a long time, turbulence and diffusion in the atmosphere are newer research areas [1]. There are some studies that predict nitrogen oxide formation from the combustion chamber [2] or determining excess air for the combustion process by employing artificial neural network [3]. But these studies do not account for the imission after the release from the stack.

\*Corresponding author.

\*E-mail address: kuzul@itu.edu.tr



Today, modeling the distribution of a pollutant is carried out with several basic mathematical algorithms: box model, Gaussian model, Eulerian model and Lagrangian model. Gaussian models, the most common mathematical models used for distribution in the atmosphere, assume that the pollutant will disperse according to a normal statistical distribution. Eulerian models solve the conservation of continuity, momentum, and mass equation for a given pollutant. The wind field vector normally used is considered turbulent and affects the pollutant concentration. Direct solution of the equation is laborious and therefore various approaches to the turbulent properties of the flow have been included. Lagrangian models predict pollutant distribution based on a reference grid that usually varies based on the prevailing wind direction or vector or the general direction of dust cloud movement. These models are generally suitable for simulating the distribution of dust with a latent form of the pollutant [4].

The AERMOD model was developed through a collaboration between the American Meteorological Society (AMS) and the United States Environmental Protection Agency (USEPA) Regulatory Model Development Committee (AERMIC) formed in 1991. On April 21, 2000, EPA proposed adopting AERMOD as the preferred regulatory model for simple and complex terrain, and it was formally adopted on November 9, 2005, becoming effective December 9, 2005. The development and acceptance process took 14 years in total [5].

The AERMOD model consists of three main modules. The first module is a steady-state dispersion model that simulates the distribution of air pollutants from stationary industrial sources over short distances of up to 50 kilometers. The second module is a meteorological data preprocessor called AERMET. This module calculates the atmospheric parameters required for the dispersion model by processing surface meteorological data, upper air soundings and data from instrument towers. The third module is AERMAP, which provides the relationship between terrain features and the behavior of air pollution plumes and simulates the effects of airflow over the terrain. In addition, the model includes an algorithm called PRIME, which is used to model the effects of downwash from pollution plumes flowing over nearby buildings. The integrated structure of these modules makes AERMOD an effective tool for air pollution analysis [5].

AERMOD, an advanced plume model, includes updated applications of boundary layer theory, understanding of turbulence and dispersion, and includes consideration of terrain interactions. It was evaluated using 10 databases, including those from flat and elevated terrain areas, urban and rural areas, and a mixture of routine monitoring networks with a limited number of fixed monitoring areas as well as tracer experiments [6].

AERMOD shows superior performance in predicting high limit concentrations compared to other applied models. Accurate and detailed input data is required for the model to work successfully. The quality of data inputs and the

model's ability to accurately reflect physical processes increases its ability to reproduce the distribution of observations. These conditions are important to understand when AERMOD can perform best under different scenarios and environmental conditions, and effective use of the model requires considering these conditions as well as the limits and requirements of the model [7].

AERMOD's meteorological preprocessor (AERMET) evaluates the structure and growth of the planetary boundary layer (PBL) based on surface effects, dependent on heat and momentum fluxes. The depth of this layer and the distribution of pollutants within it are influenced at the local scale by surface characteristics such as surface roughness, albedo, and available surface moisture. AERMOD uses surface and mixed layer scaling to characterize the structure of the PBL. AERMET uses surface characteristics, cloud cover, morning upper air temperature scanning, and near-surface measurement of wind speed, wind direction, and temperature as input. With these data, the model calculates the friction velocity, Monin-Obukhov length, convective velocity scale, temperature scale, mixing height and surface heat flux [8].

This information is necessary for the model to accurately predict how and where pollutants will spread into the atmosphere. While surface data enables the model to understand meteorological conditions at ground level, additional data provided by AERMET helps the model understand how conditions in the atmosphere change with altitude. This comprehensive data set allows the model to be more accurate and effective in air quality predictions.

Scientific review of ADMS and AERMOD technical documentation shows that many of their components are based on similar state-of-the-art algorithms; both assume a bimodal distribution of turbulent vertical velocities for convective conditions. On the other hand, ISC3 represents the typical Gaussian model that has been widely used for 30 years. It works relatively fast compared to AERMOD ADMS, which has improvements such as processing of terrains. The downstream algorithm in AERMOD does not differ from that in ISC3; whereas the downstream algorithm in ADMS is based on recent wind tunnel experiments and model developments. ADMS is unique in that it can model the transport and distribution of instantaneous oscillations. There are a few differences in input meteorology requirements, as AERMOD will allow vertical wind and temperature profiles to be entered, whereas ADMS only requires input of near-ground observations at some level. Since some components of AERMOD and ADMS are relatively new, it seems necessary to perform a series of sensitivity tests with a wide range of sources, meteorological and terrain conditions to ensure that the solutions are robust [9].

ISC3 requires determining whether the area surrounding a facility is rural or urban, thus creating a set of horizontal and vertical distribution curves (Pasquill-Gifford for rural or McElroy-Pooler for urban). There are no intermediate or other distribution ratios used. AERMOD and ADMS can include surface conditions such as soil moisture (using the Bowen ratio or Priestley parameter), surface albedo (for net

radiation estimates), and surface roughness. Surface roughness affects the vertical profiles of wind and temperature and dispersion rates in the surface layer and is an important variable in assessing dispersion around refineries and other industrial areas [9].

ISC3 uses routine meteorological data to calculate the height of the well-mixed layer. As the smoke rises less than the mixing height, the cloud becomes 'trapped' and continues to mix within the layer by reflection. Once the smoke rises above the mixing height, it can no longer spread to the ground. ADMS and AERMOD contain algorithms that measure the partial penetration of the amplified smoke cloud. Ground-level dispersion depends on on the reversal force and the buoyancy force of the smoke. This parameterization is important for very mobile clouds or moderately mobile clouds interacting with relatively low-level inversions [9].

A study conducted in 2007 compares the performance of AERMOD and ISC air distribution models and their PRIME versions in two realistic areas. The study shows that ISC predicts higher air concentrations than AERMOD in areas closer to the study area, but the predictions become more similar as distance increases. It has been found that the largest differences are generally seen in 1-hour average periods. It has been assessed that AERMOD and AERMOD-PRIME tend to predict lower concentrations than ISC [10].

In a 2006 study, field odor sampling data were used to evaluate CALPUFF and ISCST3 Gaussian distribution models to estimate downwind concentrations and back-calculate field-borne odor emission rates. According to this study, CALPUFF could predict mean downwind odor concentrations well, whereas ISCST3 tended to underpredict odor concentration compared to field measurements. Additionally, both CALPUFF and ISCST3 models failed to predict peak odor concentrations using constant mean emission from field measurements [11].

Also, in a study conducted in 2016, AERMOD and CALPUFF air distribution models were used to examine the four-season distribution of SO<sub>2</sub> emitted from a gas refinery. The models' predictions were compared with real data collected at monitoring stations, and as a result of this comparison, it was determined that CALPUFF generally performed better than AERMOD. In particular, CALPUFF predicted higher concentrations than AERMOD over certain time periods and in short-term simulations. Additionally, it has been found that AERMOD may contain some significant errors due to its sensitivity to surface features and land use, whereas CALPUFF performs better in complex terrain conditions [12].

In a study conducted in 2009, PM10 concentrations measured in a feedlot in Texas were evaluated using ISCST3 and AERMOD air distribution models. Analyzes under night conditions showed that AERMOD predicted values three times higher than measured concentrations. A sampling study conducted to determine PM concentrations in cotton pickers and the analysis of these data using the AERMOD

**Table 1.** Coordinates of the study area

Corner number	Geographical coordinates (UTM 35T)	
	Latitude	Longitude
1	577468	4543970
2	577571	4534003
3	587477	4544090
4	587583	4534118

model are also discussed. AERMOD was found to predict 1.8 times higher Emission Factors (EF) than the ISCST3 model [13]. LNG powered ship emissions were calculated for NO<sub>x</sub> [14, 15] but their modelling was not executed. A study calculated ground-level NO<sub>x</sub> emissions from an LNG plant in Oman by CALPUFF [16].

In this study, we used AERMOD, the proposed model by USEPA to calculate the ground-level NO<sub>x</sub> concentrations. This study gave us the opportunity to determine the contribution of a liquefied natural gas facility over a mid-populated district.

## MATERIALS AND METHODS

### Study Area

The study area encompasses various potential emission sources, including two port facilities specializing in the transport of liquid fuel, one port facility dedicated to dry cargo transportation, and two liquid fuel storage facilities. Additionally, the region hosts two natural gas cycle power plants contributing to the emissions landscape. Urban emission sources, such as vehicle traffic and fuel utilization for heating and cooking purposes, form another significant component. Furthermore, agricultural activities and the operations of small-scale industrial enterprises in the area contribute to the overall emissions scenario.

The modeling area was determined as 10 km x 10 km, with the center of the area being the liquefied natural gas facility. The facility in question is located within the borders of Tekirdağ's Marmaraereğlisi district and the modeling area also includes the district center. The coordinates of the study area are given in Table 1 and the study area is shown in Figure 1.

While selecting the study area, care was taken to ensure that the settlements located near the facility remained within the study area. Meteorological station number 19343, where meteorological data is taken, is also shown in Figure 1. The station in question remains within the boundaries of the study area.

### Liquefied Natural Gas Facility

The facility is one of Turkey's important energy infrastructure facilities and is located 85 km from Istanbul, 40 km from Tekirdağ, 20 km from Çorlu Airport and 4 km from Marmara Ereğlisi district centre. The terminal started its journey with the basic design studies that started in 1985,



**Figure 1.** Map of the study area.

construction works started in 1989 and was completed and put into service in 1994. Capacity increase in 2001, filling operations for land tankers and pier expansion works started in 2007 and were completed in 2016. Finally, the terminal's gas sending capacity was increased in 2018.

The main functions of the terminal include unloading and storage from LNG vessel, gasification of stored LNG and delivery of natural gas to the main transmission line and land tanker filling. Design capacity is 37 million Nm<sup>3</sup>/day. The terminal has three LNG storage tanks with a total capacity of 255,000 m<sup>3</sup>.

LNG gasification and shipping processes include taking the stored LNG from tanks and sending it via pipeline to the main transmission line 23 km away after natural gas measurement. The land tanker filling ramp is used to send natural gas to regions where natural gas cannot be delivered via pipeline and has a daily filling capacity of 75 tankers.

A significant portion of the facility's emissions come from natural gas submerged combustion vaporizers (SCV) and flare chimneys. SCVs are used to gasify the liquefied natural gas stored in the facility by heating it. This equipment uses natural gas as fuel. Flare chimneys ensure that natural gas is burned and discharged into the atmosphere during sudden pressure increases in the facility.

#### Determination of Mass Emissions

Five-point emission sources have been determined for the facility: SCV A, SCV B, SCV C, SCV D, and flare chimneys. Consumption of each point source was determined based on the values obtained by reading the flowmeters. Consumption data is in Table 2.

Apart from the consumption under normal operating conditions, the consumption values of these equipment have been determined from their catalogs for the scenarios in which the equipment will operate at full capacity and at minimum capacity. (For SCVs, maximum consumption = 3244 Sm<sup>3</sup>/hour, minimum consumption = 220 Sm<sup>3</sup>/hour)

To determine the NO<sub>x</sub> emissions resulting from these stacks, the emission measurement that the facility must have in accordance with environmental legislation was used to find the mass emission rates. The mass flow rate value was calculated by dividing the mass concentration measurement data from stack to the volumetric flowrate measured at the stack. When mass emission is divided by the consumption of LNG, the emission factor is calculated. NO<sub>x</sub> emission factor was found to be 92.765 mg/Nm<sup>3</sup>. Mass emission data is included in Table 3.

#### Data Used by AERMOD Application in the Study

Five-point emission sources have been determined for the facility: SCV A, SCV B, SCV C, SCV D and flare chimneys. Data on emission sources are given in Table 4.

Using the AERMOD modeling system, pollutant concentrations were calculated at ground level every 500 meters from the starting point to 10,000 m.

In the study, the hourly surface data required by the model (wind speed, wind direction, temperature and cloud cover, etc.) were obtained from the Tekirdağ Marmaraereğlisi station affiliated with the General Directorate of State Meteorological Affairs for 2022. Upper air data was taken from radiosonde data at Istanbul Kartal station, which is the closest point to the study area. The wind frequency rose, including wind speeds and wind directions for 2022, is shown in Figure 2.

**Table 2.** Consumption values

Months	Volumetric flowrates (Sm <sup>3</sup> )				
	SCV A	SCV B	SCV C	SCV D	Flare
J	0	0	0	0	98.586
F	0	2.844	29.623	126.787	102.378
M	0	72.992	15.167	71.096	121.337
A	0	0	150.426	148.356	97.638
M	0	0	2.398	12.797	78.679
J	92	0	449	0	54.981
J	14.598	127.972	75.362	35.548	59.720
A	137.524	323895	307457	187882	52137
S	0	39.870	83	0	67304
O	629	10.359	53.629	9.389	55929
N	478	11.192	218.128	0	109961
D	0	0	0	0	99534

AERMET is a data processor and preprocessor that prepares meteorological data for AERMOD. This process involves first collecting data from appropriate meteorological data sources and subjecting these data to quality control. Quality control increases the reliability of the dataset and the accuracy of the model. Then, the collected data is converted into a usable format by AERMET and the meteorological fields (temperature, wind speed and direction, humidity, etc.) needed by the air quality model are created. In the final stage, the processed meteorological data are presented in a format that can be used by air quality models.

The data AERMET requires include items such as temperature, wind speed and direction, humidity, cloudiness, sunlight, amount and type of precipitation, atmospheric pressure. Additionally, specific data such as local geography and land use are also important to improve the accuracy of the models.

The reliability of the model results can be assessed through quantile-quantile (Q-Q) plots. These can be generated by plotting measured data against modelled data. There are some studies which served for this purpose and showed good agreement between measured and predicted concentrations [5, 17].

**RESULTS AND DISCUSSION**

A modeling study was carried out using three different scenarios on the distribution of NO<sub>x</sub> emissions originating from and potentially arising from Marmaraeğlisi LNG Terminal. Calculations were made using the AERMOD program for 441 receptor points. Two different time averages used to generate figures for each scenario. In the first, the maximum daily concentrations at each of the points. In the second, the average values of the concentrations calculated throughout the year. These time averages were used to generate figures for three different scenarios. These sce-

**Table 3.** Mass emission rates

Months	Mass flowrates				
	SCV A (g/s)	SCV B (g/s)	SCV C (g/s)	SCV D (g/s)	Flare (g/s.m <sup>2</sup> )
J	-	-	-	-	0.00683
F	-	0.00011	0.00114	0.00486	0.00785
M	-	0.00253	0.00053	0.00246	0.00840
A	-	-	0.00538	0.00531	0.00699
M	-	-	0.00008	0.00044	0.00545
J	0.00001	-	0.00002	0.00000	0.00394
J	0.00051	0.00443	0.00261	0.00123	0.00414
A	0.00476	0.01122	0.01065	0.00651	0.00361
S	-	0.00143	0.00001	-	0.00482
O	0.00002	0.00036	0.00186	0.00033	0.00387
N	0.00002	0.00040	0.00781	-	0.00787
D	-	-	-	-	0.00689

**Table 4.** Data of emission sources

Source name	Temperature (°K)	Stack gas velocity (m/s)	Stack diameter (m)	Stack height (m)
SCV A	291.55	6.41	0.8	10
SCV B	292.25	6.55	1.2	10
SCV C	291.82	7.41	1.2	10
SCV D	290.72	6.77	1.2	10
Flare	-	-	1.2	60

narios for the facility are as follows: In the first scenario, it is assumed that the facility will operate under normal operating conditions, in the second scenario, it is assumed that the equipment and points determined as emission sources will consume maximum natural gas, and in the third and last scenario, it is assumed that the emission sources will consume natural gas at a minimum level.

**NO<sub>x</sub> Concentrations in Operating Conditions**

The first calculations estimated the maximum of 24-hour average concentrations. The highest concentration in the study area was observed to be 1.70 µg/m<sup>3</sup> on 09.08.2022. The lowest concentration was determined to be >0.01 µg/m<sup>3</sup> on 27.04.2022. The highest 24-hour average concentrations are found in Figure 3. When the map is examined, it is seen that the highest concentrations are in the facility area. According to the distribution map, it is clearly seen that the pollutants are transported in the direction of the prevailing wind as seen in Figure 2.

Additionally, annual average concentrations were calculated as a result of the modeling study conducted at 441 points. It was observed that the highest concentration average in the study area was 0.11 µg/m<sup>3</sup>. The lowest concentration average was found to be >0.01 µg/m<sup>3</sup>. Annual

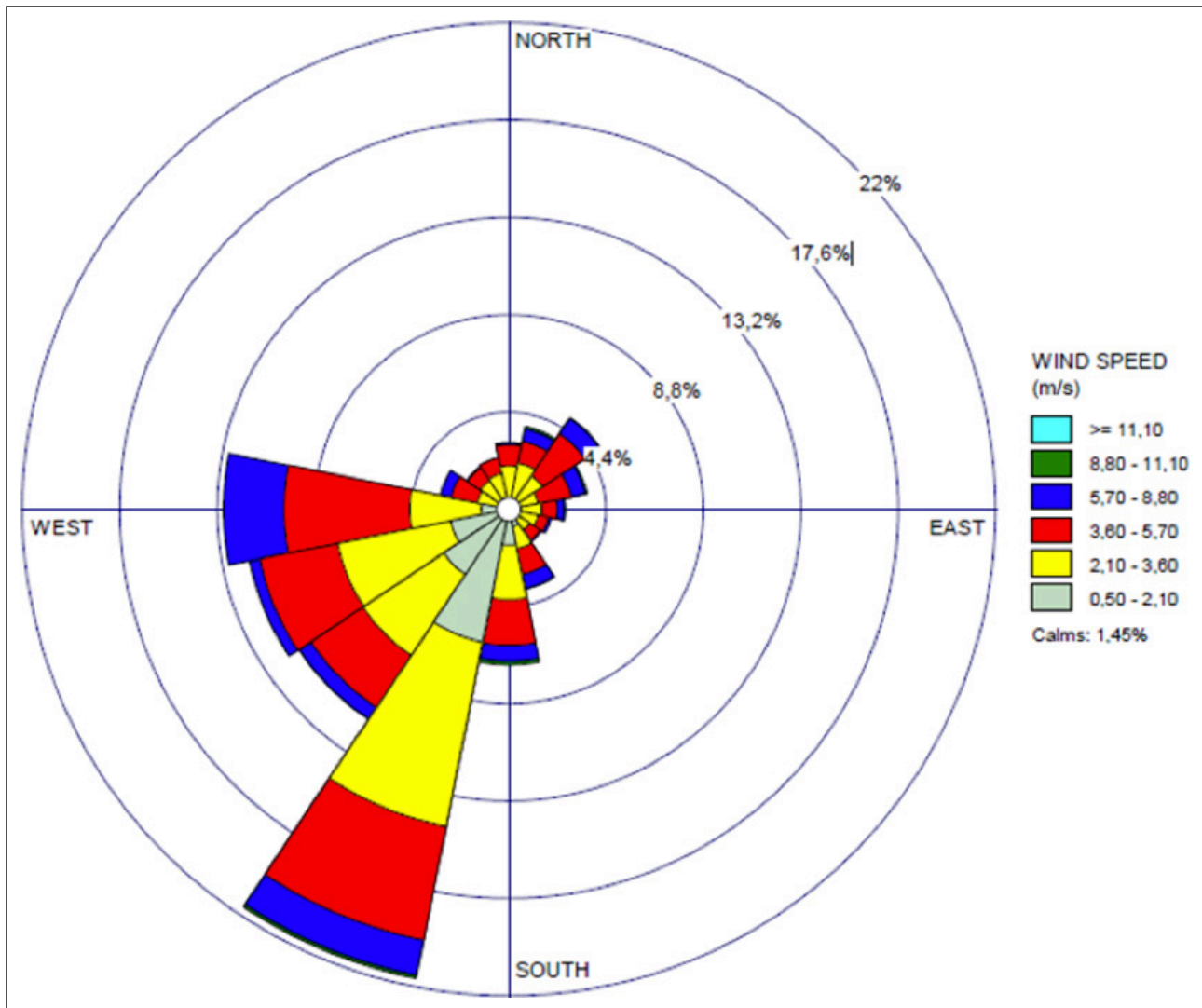


**Figure 2.** Windrose plot of 2022 for Marmaraereğlisi.

average concentrations are found in Figure 4. When the map is examined, it is seen that the highest concentrations are in the facility area.

#### **NO<sub>x</sub> Concentrations at Maximum Operation Capacity**

For the situation where the facility operates at maximum capacity throughout the year, the maximum 24-hour concentration averages were found. The highest concentration in the study area was observed to be 16.24  $\mu\text{g}/\text{m}^3$  on 09.08.2022. The lowest concentration was determined to be 0.06  $\mu\text{g}/\text{m}^3$  on 25.02.2022. The highest 24-hour average concentrations are found in Figure 5. When the map is examined, it is seen that the highest concentrations are in the facility area.

Annual average concentrations were calculated and it was observed that the highest concentration average in the study area was 2.51  $\mu\text{g}/\text{m}^3$ . The lowest concentration average was found to be >0.01  $\mu\text{g}/\text{m}^3$ . Annual average concentrations are found in Figure 6. When the map is examined, it is seen that the highest concentrations are in the facility area.

#### **NO<sub>x</sub> Concentrations at Minimum Capacity**

For the scenario with minimum operation capacity throughout the year, the maximum 24-hour concentration averages were calculated. The highest concentration in the study area was observed to be 1.11  $\mu\text{g}/\text{m}^3$  on 09.08.2022. The lowest concentration was determined to be >0.01  $\mu\text{g}/\text{m}^3$  on 25.02.2022. The highest 24-hour average concentrations are found in Figure 7. When the map is examined, it is seen that the highest concentrations are in the facility area.

Additionally, annual average concentrations were calculated as a result of the modeling study conducted at 441 points. It was observed that the highest concentration average in the study area was 0.17  $\mu\text{g}/\text{m}^3$ . The lowest concentration average was found to be >0.01  $\mu\text{g}/\text{m}^3$ . Annual average concentrations are found in Figure 8. It can be inferred that the highest concentrations are in the facility area.

The escalating severity of air pollution poses a substantiated threat to ecosystems, as evidenced by numerous studies. Heightened levels of pollution intensify apprehensions regarding future implications. Factors such

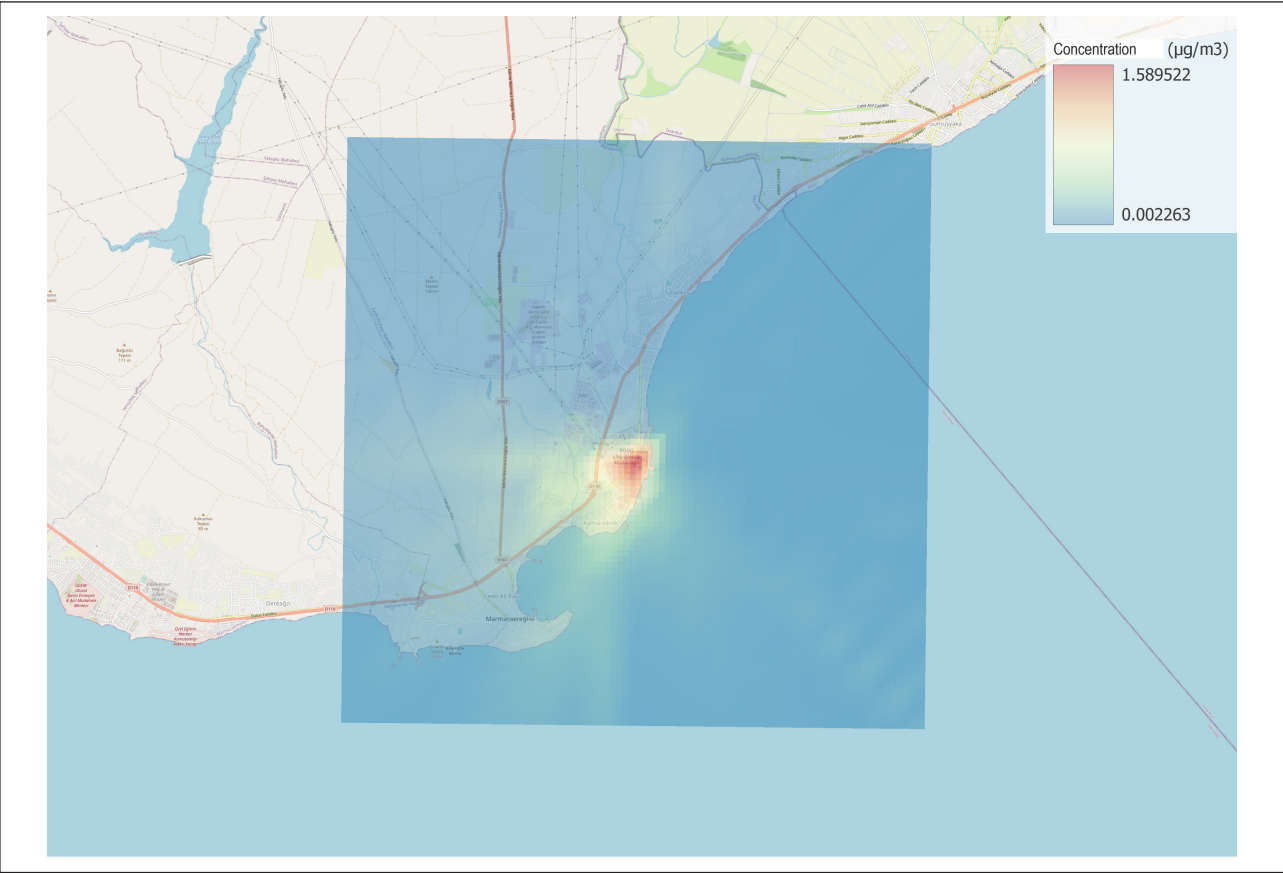


Figure 3. Maximum daily concentrations at operation conditions.

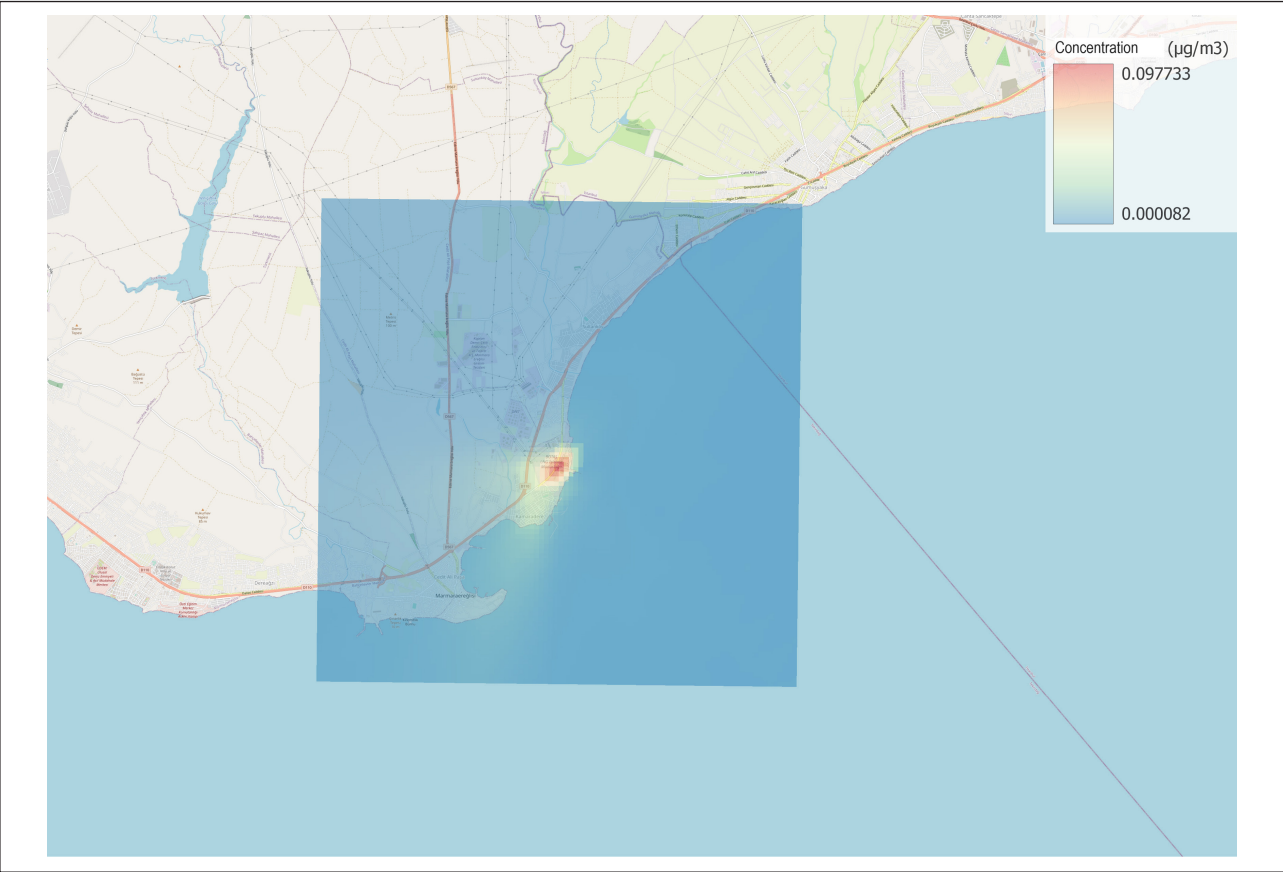


Figure 4. Annual average concentrations at usual operation capacity.

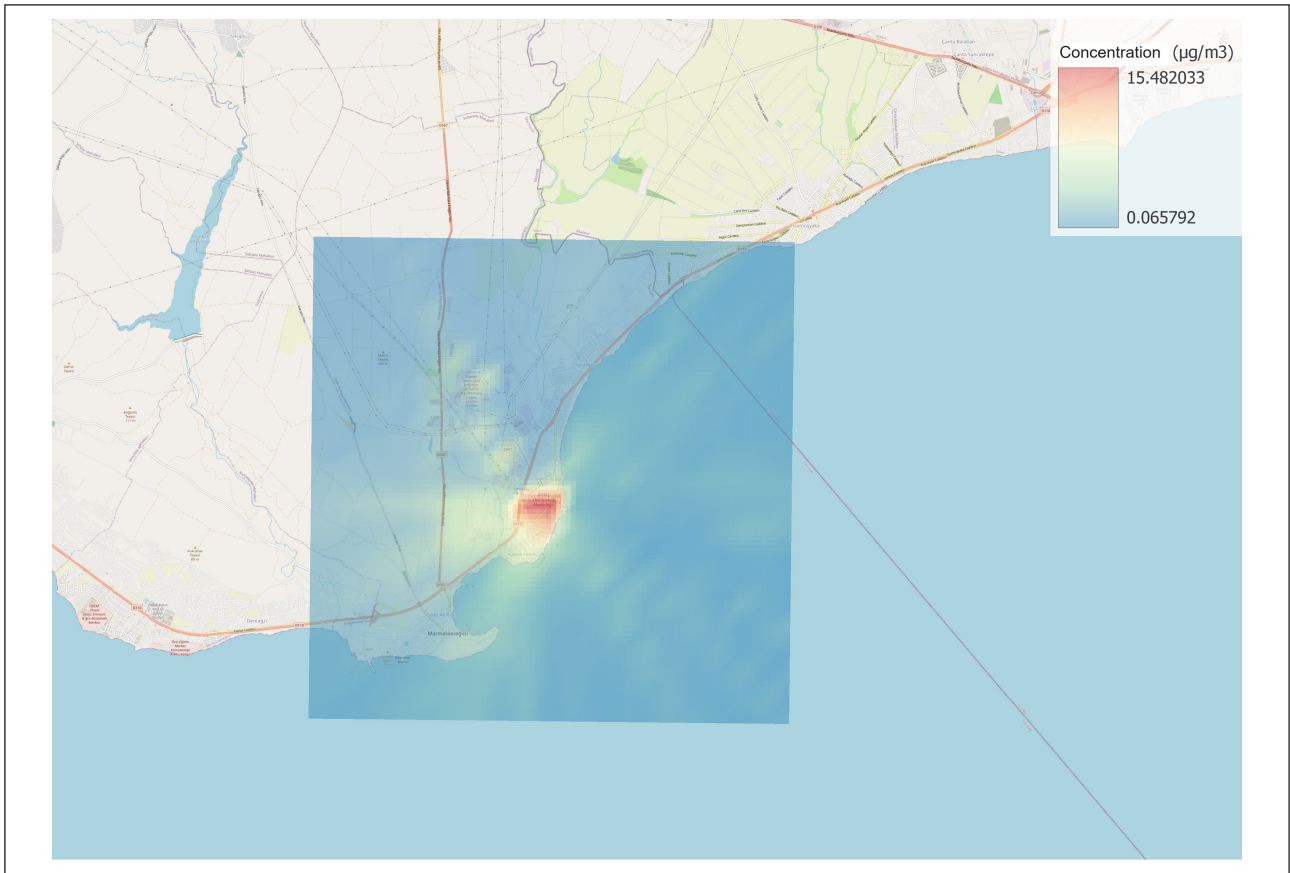


Figure 5. Daily maximum NO<sub>x</sub> concentrations during maximum operation conditions.

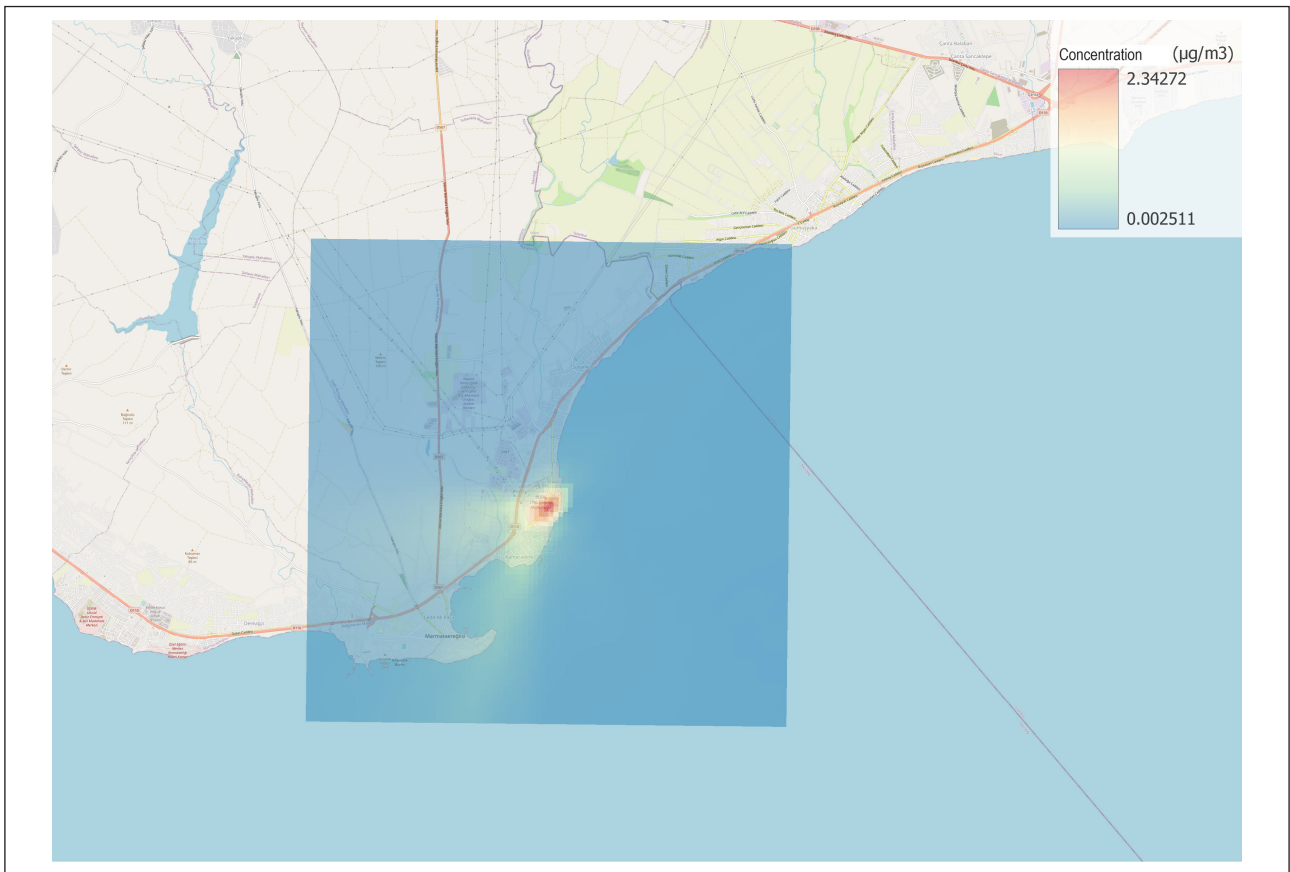


Figure 6. Annual NO<sub>x</sub> concentrations during maximum operation conditions.



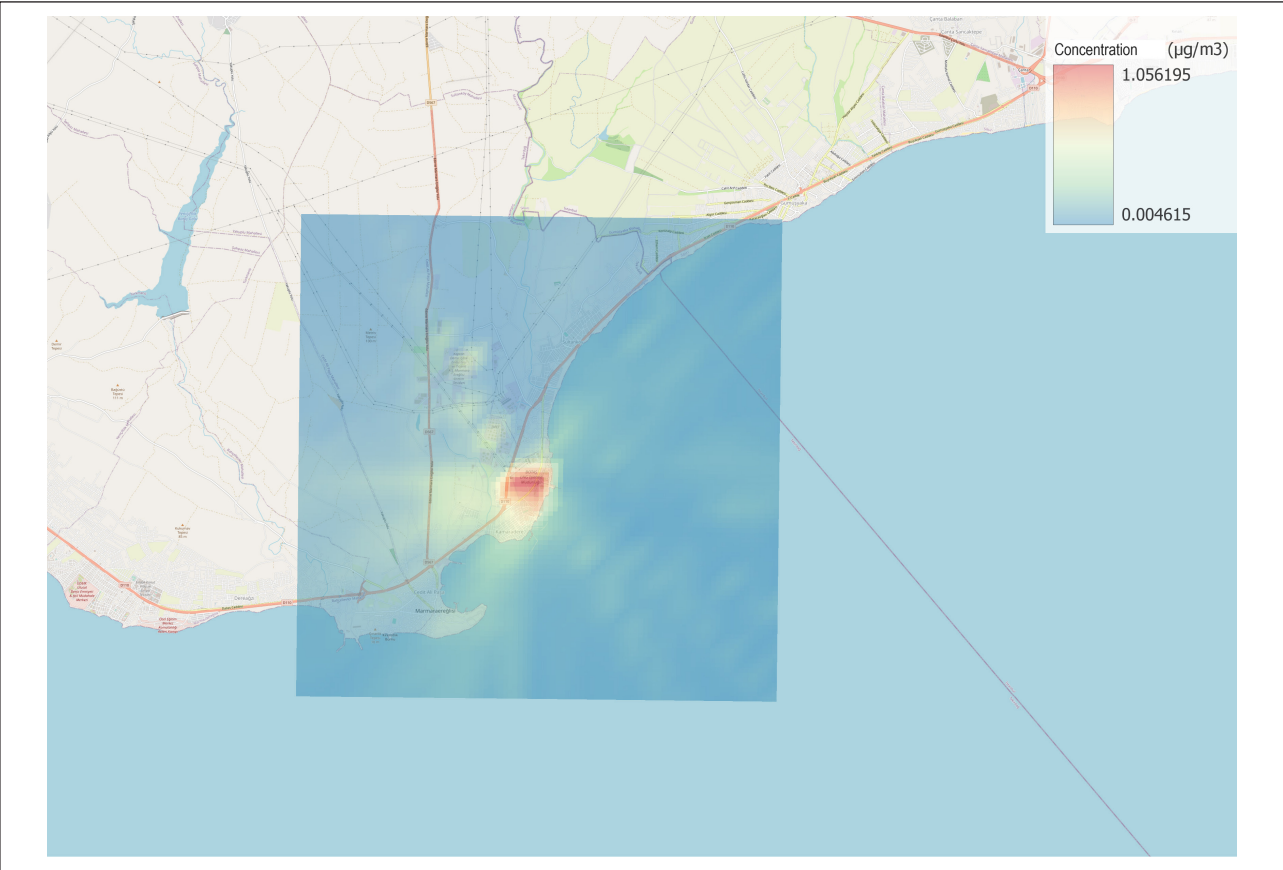


Figure 7. Daily maximum NO<sub>x</sub> concentrations during minimum operation conditions.

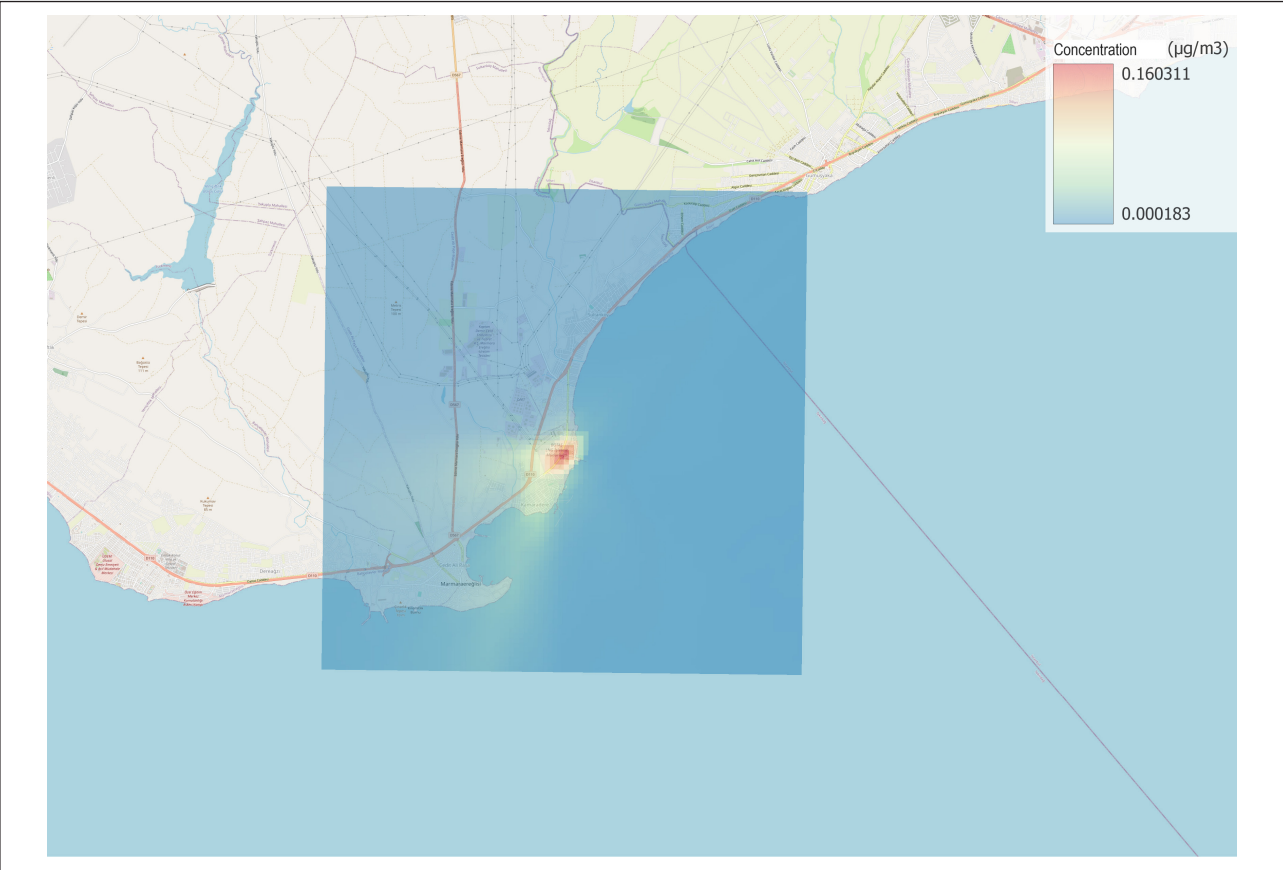


Figure 8. Annual NO<sub>x</sub> concentrations during minimum operation conditions.

as burgeoning global population, industrial expansion, unregulated urban development, and escalating energy demands contribute to the exacerbation of air pollution. Consequently, it has become imperative to conduct comprehensive assessments for both newly established and existing facilities to ascertain effective mitigation strategies for combating air pollution.

In this study, emissions from an LNG facility were modeled using AERMOD. The reason for choosing this model is that the required data is at a minimum level and the run time of the model is extremely short. The topography of the area to be modeled is also an extremely important element in model selection. When the AERMOD model is used, reliable results may not be obtained for areas with complex terrain structure. However, AERMOD is a suitable choice since the land structure of the area chosen for the study is quite flat.

When the data obtained through the model is evaluated in terms of the air quality legislation of Türkiye, it is seen that the ground-level concentrations resulting from the facility remain below the limit values. Even if the facility operates at maximum capacity, the highest 24-hour average  $\text{NO}_x$  concentration would be detected as  $16.24 \mu\text{g}/\text{m}^3$ . The compared legislation is the Regulation on the Control of Industrial Air Pollution, published in the Official Gazette dated 03.07.2009 and numbered 27277 [18]. The data compared with the value in table 5.1 inside the legislation. It is in accordance with the European Directive [19]. Air quality standard is met in terms of  $\text{NO}_x$ . When the annual average concentrations for the maximum capacity scenario is considered, the highest expected concentration would be  $2.51 \mu\text{g}/\text{m}^3$ . This also remains below the long-term limit value determined in the same regulation. The  $\text{NO}_2$  limit values are 350, 125, 60, and  $25 \mu\text{g}/\text{m}^3$  for hourly, daily, long-term, and winter-time concentrations, respectively.

A study was conducted in Oman around LNG plant to measure air pollutant concentrations [20]. The annual mean was 21.29 ppb for  $\text{NO}_2$ . Air quality standards were not exceeded for  $\text{NO}_2$ . But this is a cumulative concentration value and does not only consider the plant. It has contribution from all surrounding sources. A modelling study was conducted for the same facility [21]. The highest hourly concentrations were calculated as  $2027.4 \mu\text{g}/\text{m}^3$  and  $625.54 \mu\text{g}/\text{m}^3$  for winter and summer seasons, respectively. A simple Gaussian model was applied in Nigeria to calculate ground-level concentrations downwind of an LNG plant [22]. According to different scenarios,  $\text{NO}_x$  concentrations varied between 2.12 and  $27.83 \mu\text{g}/\text{m}^3$ . There is an agreement with this study to our results.

Previous studies showed that significantly more concentrations above the shoreline can be achieved in the places where are close to ports. Ekmekçiöğlü et al. [23] determined up to  $100 \mu\text{g}/\text{m}^3$  annual average  $\text{NO}_x$  concentration in Kocaeli, on the other hand, they reported annual average  $\text{NO}_x$  concentration in Ambarlı (Istanbul) around  $10 \mu\text{g}/\text{m}^3$ . Kuzu et al. [24] found that annual average  $\text{NO}_x$  concentrations were as high as  $520 \mu\text{g}/\text{m}^3$  in Bandırma, which is a district located around a port. Close to the value found in Bandırma, Kuzu

[25] estimated an annual maximum at Atatürk International Airport, with a value of  $560 \mu\text{g}/\text{m}^3$ . Compared to those reported previous values, the contribution from LNG facility seems quite limited to  $\text{NO}_x$  concentrations.

## CONCLUSIONS

Upon evaluation of the findings, it is evident that the adverse impacts of the liquefied natural gas facility on the environment and nearby settlements are notably minimal. A crucial takeaway from this investigation underscores the necessity of conducting comprehensive integrated assessments for settlements. While current legislative frameworks and practices typically focus on evaluating individual facilities' impacts on air pollution, this approach alone is insufficient. The efficacy of assessing other emission sources such as industrial facilities, traffic, and heating sources concurrently within the regions earmarked for facility establishment holds greater promise in shaping air quality. The primary limitation of the study is that the modeling only includes encompasses the impacts of the liquefied natural gas facility, potentially overlooking broader environmental considerations when it is compared to the legislation limits. However, the value can be exceeded in the atmosphere. The authors recommend expanding the study by including other local emissions to make a comprehensive modelling in the district. Additionally, marine boundary layer development can be considered in another study.

## DATA AVAILABILITY STATEMENT

The author confirm that the data that supports the findings of this study are available within the article. Raw data that support the finding of this study are available from the corresponding author, upon reasonable request.

## CONFLICT OF INTEREST

The author declared no potential conflicts of interest with respect to the research, authorship, and/or publication of this article.

## USE OF AI FOR WRITING ASSISTANCE

Not declared.

## ETHICS

There are no ethical issues with the publication of this manuscript.

## REFERENCES

- [1] A. Daly, and P. Zannetti, "Air pollution modeling—An overview," in Ambient air pollution P. Zannetti, D. Al-Ajmi, and S. Al-Rashied, The Arab School for Science and Technology (ASST) and The Enviro-Comp Institute, 2007, pp. 15–28.
- [2] S. Golgiyaz, M. Daskin, C. Onat, M.F. Talu, "An artificial intelligence regression model for prediction of nox emission from flame image," Journal of Soft

- Computing and Artificial Intelligence, Vol. 3, pp. 93–101, 2022. [CrossRef]
- [3] S. Golgiyaz, M.F. Talu, M. Daskin, and C. Onat, “Estimation of excess air coefficient on coal combustion processes via gauss model and artificial neural network,” Alexandria Engineering Journal, Vol. 61, pp. 1079–1089, 2022. [CrossRef]
- [4] K. E. Kakosimos, M. J. Assael, J. S. Lioumbas, and A. S. Spiridis, “Atmospheric dispersion modelling of the fugitive particulate matter from overburden dumps with numerical and integral models”, Atmospheric Pollution Research, Vol. 2, pp. 24–33, 2011. [CrossRef]
- [5] US EPA (2018). User’s Guide for the AMS/EPA Regulatory Model (AERMOD), US Environmental Protection Agency, EPA-454/B-18-001, RTP, NC.
- [6] R. J. Paine, R. F. Lee, R. W. Brode, R. Wilson, A. J. Cimorelli, S. G. Perry, J. C. Weil, A. Venkatram, and P. Peters, (1999). “AERMOD: MODEL FORMULATION AND EVALUATION RESULTS”, Proceedings of the 92nd Annual Meeting of the Air & Waste Management Association, St. Louis, MO, June 20–24, 1999.
- [7] S. G. Perry, A. J. Cimorelli, R. J. Paine, R. W. Brode, J. C. Weil, A. Venkatram, R. B. Wilson, R. F. Lee, and W. D. Peters, “AERMOD: A dispersion model for industrial source applications. part ii: model performance against 17 field study databases,” Journal of Applied Meteorology, Vol. 44(5), pp. 694–708, 2005. [CrossRef]
- [8] A. J. Cimorelli, S. G. Perry, A. Venkatram, J. C. Weil, R. Paine, R. B. Wilson, R. F. Lee, W. D. Peters, R. and W. Brode, (2005). “AERMOD: A dispersion model for industrial source applications. part i: general model formulation and boundary layer characterization,” Journal of Applied Meteorology, Vol. 44(5), pp. 682–693, 2005. [CrossRef]
- [9] S. R. Hanna, B. A. Egan, J. Purdum, and J. Wagler, “Evaluation of the ADMS, AERMOD, and ISC3 dispersion models with the OPTEX, Duke Forest, Kincaid, Indianapolis and Lovett field datasets,” International Journal of Environment and Pollution, Vol. 16(1-6), pp. 301–314, 2021. [CrossRef]
- [10] K. C. Silverman, J. G. Tell, E. V. Sargent, and Z. Qiu, “Comparison of the industrial source complex and aermოდ dispersion models: case study for human health risk assessment,” Journal of the Air & Waste Management Association, Vol. 57(12), pp. 1439–1446, 2007. [CrossRef]
- [11] L. Wang, D. Parker, C. Parnell, R. Lacey, and B. Shaw, “Comparison of CALPUFF and ISCST3 models for predicting downwind odor and source emission rates,” Atmospheric Environment, Vol. 40(25), pp. 4663–4669, 2006. [CrossRef]
- [12] F. Atabi, F. Jafarigol, F. Moattar, and J. Nouri, “Comparison of AERMOD and CALPUFF models for simulating SO<sub>2</sub> concentrations in a gas refinery,” Environmental Monitoring and Assessment, Vol. 188(9), Article 516, 2016. [CrossRef]
- [13] V. S. V. Botlaguduru, “Comparison of Aermოდ and ISCST3 Models For Particulate Emissions From Ground Level Sources,” Master dissertation, Texas A&M University, College Station, TX, 2009.
- [14] Y. Afon, and D. Ervin, “An assessment of air emissions from liquefied natural gas ships using different power systems and different fuels”, Journal of The Air & Waste Management Association, Vol. 58, pp. 404–411, 2008. [CrossRef]
- [15] M. Anderson, K. Salo, and E. Fridell, “Particle- and Gaseous Emissions from an LNG Powered Ship”, Environmental Science and Technology, Vol. 49(20), pp. 12568–12575, 2015. [CrossRef]
- [16] S. A. Abdul-Wahab, S. O. Fadlallah, M. Al-Riyami, and I. Osman, “A study of the effects of CO, NO<sub>2</sub>, and PM<sub>10</sub> emissions from the Oman Liquefied Natural Gas (LNG) plant on ambient air quality,” Air Quality, Atmosphere, and Health, Vol. 13, pp. 1235–1245, 2020. [CrossRef]
- [17] A. ul Haq, Q. Nadeem, A. Farooq, N. Irfan, M. Ahmad, and M. R. Ali, “Assessment of AERMOD modeling system for application in complex terrain in Pakistan,” Atmospheric Pollution Research, Vol. 10, pp. 1492–1497, 2019. [CrossRef]
- [18] Sanayi Kaynaklı Hava Kirliliğinin Kontrolü Yönetmeliği, Resmi Gazete, 29211. Available at: Dec 20, 2014. (Turkish legislation)
- [19] European Directive. “Directive 2008/50/EC of the European Parliament and of the Council of 21 May 2008 on ambient air quality and cleaner air for Europe.”, Directive 2008/50/EC, air quality, 2008.
- [20] S. A. Abdul-Wahab, “Monitoring of air pollution in the atmosphere around oman liquid natural gas (OLNG) plant,” Journal of Environmental Science and Health, Vol. 40(3), pp. 559–570, 2005. [CrossRef]
- [21] S. A. Abdul-Wahab, S. O. Fadlallah, M. Al-Riyami, M. Al-Souti, and I. Osman, “A study of the effects of CO, NO<sub>2</sub>, and PM<sub>10</sub> emissions from the Oman Liquefied Natural Gas (LNG) plant on ambient air quality,” Air Quality, Atmosphere and Health, Vol. 13, pp. 1235–1245, 2020. [CrossRef]
- [22] P. N. Ede, D. O. Edokpa, and O. Ayodeji, “Aspects of air quality status of bonny island, Nigeria attributed to an LNG plant,” Energy and Environment, Vol. 22, pp. 891–909, 2011. [CrossRef]
- [23] A. Ekmekçioğlu, S. L. Kuzu, K. Ünlügençoğlu, and U. B. Çelebi, “Assessment of shipping emission factors through monitoring and modelling studies,” Science of the Total Environment, Article 140742, 2020. [CrossRef]
- [24] S. L. Kuzu, L. Bilgili, and A. Kılıç, “Estimation and dispersion analysis of shipping emissions in Bandırma Port, Turkey,” Environment, Development and Sustainability, Vol. 23, pp. 10288–10308, 2021. [CrossRef]
- [25] S. L. Kuzu, “Estimation and dispersion modeling of landing and take-off (LTO) cycle emissions from Atatürk International Airport,” Air Quality Atmosphere and Health, Vol. 11, pp. 153–161, 2018. [CrossRef]